Hindawi
Mathematical Problems in Engineering
Volume 2019, Article ID 5671361, 13 pages
https://doi.org/10.1155/2019/5671361

Research Article

Transverse Vibration of a Moving Viscoelastic Hard Membrane Containing Scratches

Mingyue Shao,[1] **Jimei Wu**,[1,2] **Yan Wang**,[3] **Hongmei Zhang**,[2] **and Qiumin Wu**[2]

[1]*School of Mechanical and Precision Instrument Engineering, Xi'an University of Technology, Xi'an 710048, China*
[2]*Faculty of Printing, Packaging and Digital Media Engineering, Xi'an University of Technology, Xi'an 710048, China*
[3]*School of Civil Engineering and Architecture, Xi'an University of Technology, Xi'an 710048, China*

Correspondence should be addressed to Jimei Wu; wujimei1@163.com

Received 26 September 2018; Accepted 9 January 2019; Published 22 January 2019

Academic Editor: Andrés Sáez

The transverse vibration and stability of a moving viscoelastic hard printing membrane containing scratches are investigated. Based on the viscoelastic differential constitutive relation, thin plate theory, and d'Alembert principle, the differential equation of a moving viscoelastic hard membrane with a straight scratch through the surface is derived by using the continuity condition of the scratches. The complex characteristic equation is obtained by using the differential quadrature method. The effects of the scratch depth and scratch position on the critical instability speed of the moving hard membrane were highlighted by solving the differential equation and numerical calculation, and the coupling effects of speed and scratch depth on vibration characteristics of the hard membrane are also analyzed. Numerical calculation results show that the hard membrane experiences divergence instability when the actual printing speed is v=23.2 m/s, and the membrane is stable when v<23.2 m/s. The theoretical guidance and method for scratches detection of the precision coated hard membrane are provided.

1. Introduction

Hard scratches are often caused by fine particles and sharp iron filings on the surface of a precision coated hard membrane. The hard membrane has a certain hardness and can take bending rigidity [1], the thin plate theory is used to analyze the hard membrane. This part of the membrane material with scratches is a waste product, which must be diagnosed and eliminated in time to ensure the quality and productivity of the printing product. The damage effect can cause changes in the dynamic characteristics of the vibration mode and frequency of the structure. Therefore, changes in dynamic characteristics can be used to identify scratch damage of the membrane structure. Therefore, it is necessary to study the vibration characteristics of a viscoelastic hard membrane containing scratches.

In the past decade, many scholars have studied the dynamic characteristics of moving viscoelastic plates. Marynowski [2] investigated moving velocity, and relaxation times affected the dynamic behavior of a moving plate based on the viscoelastic theory. Li [3] studied multimodal coupling characteristics of a moving viscoelastic sandwich rectangular plate by using the Galerkin method and the thin plate theory. Tang and Chen [4] analyzed steady-state responses of axially moving viscoelastic plates with variable speed, and the Kelvin-Voigt model was used in plate material. Pan et al. [5] analyzed the effect of thermal parameters on the transverse vibration of a viscoelastic thin plate. The conclusion is that critical divergence and restabilization speed of the first-order mode decrease with the increase of thermal parameters. Tang et al. [6] examined the vibration and dynamic stability of axially viscoelastic plates with variable tension by using the method of multiple scales and the Routh-Hurwitz criterion. Robinson and Adali [7] investigated the influence of the thickness ratio and the cross-section on the vibration of in-plane moving viscoelastic plates. The effects of aspect ratio and viscosity of plates on the vibration frequencies are presented by applying the differential quadrature method in [8]. Zheng and Deng [9] studied nonlinear free vibration of a viscoelastic moderately thick laminated plate with damage by using the

iterative methods, Newton-Cotes and Simpson integration. Marynowski [1, 10] then studied nonlinear behavior of a paper web; the viscoelastic beam theory was applied to establish the paper web model and the viscous damping was considered. He also discussed the significant influence of the tension fluctuation amplitude on the nonlinear bifurcation of the system, and the chaos and regular motion appeared alternately when the tension fluctuation amplitude increased. Zhou and Wang [11] investigated the dynamic characteristics and stability of axially moving viscoelastic thin plates by the differential quadrature method.

In recent years, scholars have conducted a lot of research on damage identification and vibration of structures with cracks. Bose and Mohanty [13] applied the Kirchhoff plate theory to analyze the vibration of a rectangular thin isotropic plate with part-through surface cracks under different boundary conditions. Diba et al. [14] analyzed the influence of parameters such as the position of excitation force, the angle of crack, and the length of crack on vibration of an isotropic rectangular plate containing an inclined crack. Wang et al. [15] employed the DQM (differential quadrature method) to analyze vibration and stability of a viscoelastic cracked plate containing changing thickness. Joshi and Jain [16] applied the classical plate theory to study the parameter vibration and thermal buckling behavior of a thin plate with internal crack. It was noted that the temperature affected natural frequencies. Joshi et al. [17] investigated the effects of boundary conditions, thickness, crack location, crack length, and varying elasticity ratio on the fundamental frequencies of a plate containing an internal crack by using Galerkin method and multiple scales perturbation method. Ramtekkar et al. [18] studied vibration and stability of plates with two perpendicular cracks, and the effects of boundary conditions and length ratios of a crack on the natural frequencies of cracked plates were analyzed.

Many studies have developed viscoelastic cracked plates with no axial moving speed, while the vibration characteristics of an axially moving viscoelastic hard membrane with cracks in the printing field have received little attention. In this paper, the dynamic properties of a viscoelastic hard membrane with scratches are studied. The theory of fracture mechanics is used to study the scratched membrane, and the complex characteristic equation of the hard membrane containing scratches is established. The influence of the scratch position and depth on the vibration and stability is analyzed. The study provides methods for scratch detection and troubleshooting identification.

2. The Differential Equation of Motion is Established

A schematic diagram of a precision coated hard membrane with a scratch is shown in Figure 1. There is a scratch at the $x = x_c$, scratch depth is h_c, and the moving hard membrane is divided into two parts by the scratch. The density of the hard membrane is ρ, the thickness is h, and the speed is v.

According to Kirchhoff's hypothesis that the strain and stress of an infinitesimal element of the hard membrane are

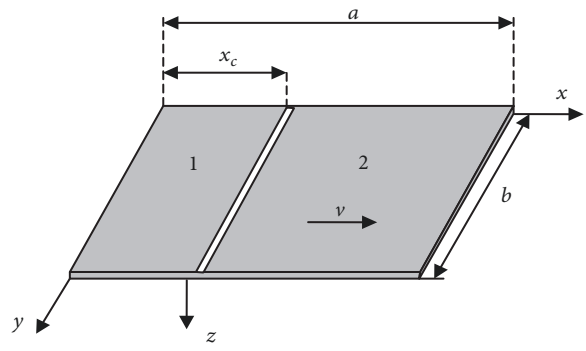

Figure 1: Hard printing membrane with a scratch.

ε_x, ε_y, ε_{xy}, σ_x, σ_y, τ_{xy}, the stress-strain relationship of a viscoelastic hard membrane is written as follows [19].

$$\begin{aligned}
&\overline{P}'\left(\overline{P}'\overline{Q}'' + 2\overline{Q}'\overline{P}''\right)\overline{\sigma}_x \\
&\quad = \overline{Q}'\left(2\overline{P}'\overline{Q}'' + \overline{Q}'\overline{P}''\right)\overline{\varepsilon}_x + \overline{Q}'\left(\overline{P}'\overline{Q}'' - \overline{Q}'\overline{P}''\right)\overline{\varepsilon}_y \\
&\overline{P}'\left(\overline{P}'\overline{Q}'' + 2\overline{Q}'\overline{P}''\right)\overline{\sigma}_y \\
&\quad = \overline{Q}'\left(\overline{P}'\overline{Q}'' - \overline{Q}'\overline{P}''\right)\overline{\varepsilon}_x + \overline{Q}'\left(2\overline{P}'\overline{Q}'' + \overline{Q}'\overline{P}''\right)\overline{\varepsilon}_y \\
&\overline{P}'\overline{\tau}_{xy} = \overline{Q}'\overline{\varepsilon}_{xy}
\end{aligned} \tag{1}$$

$\overline{P}'$, $\overline{Q}'$, $\overline{P}''$, $\overline{Q}''$ denote three-dimensional constitutive relationship.

$$\begin{aligned}
P's_{ij} &= Q'e_{ij} \\
P''\sigma_{ii} &= Q''\varepsilon_{ii}
\end{aligned} \tag{2}$$

Take Laplace transform on P', Q', P'', Q'', where "–" stands for the Laplace transform.

$$\begin{aligned}
\overline{P}' &= \sum_{k=0}^{m'} p_k' s_1^k, \\
\overline{Q}' &= \sum_{k=0}^{n'} q_k' s_1^k, \\
\overline{P}'' &= \sum_{k=0}^{m''} p_k'' s_1^k, \\
\overline{Q}'' &= \sum_{k=0}^{n''} q_k'' s_1^k
\end{aligned} \tag{3}$$

where s_1 is Laplacian variable.

Supposing that

$$\begin{aligned}
\overline{P}_0 &= \overline{P}'\left(\overline{P}'\overline{Q}'' + 2\overline{Q}'\overline{P}''\right) \\
\overline{Q}_0 &= \overline{Q}'\left(2\overline{P}'\overline{Q}'' + \overline{Q}'\overline{P}''\right) \\
\overline{Q}_1 &= \overline{Q}'\left(\overline{P}'\overline{Q}'' - \overline{Q}'\overline{P}''\right)
\end{aligned} \tag{4}$$

(1) can be expressed as follows.

$$\begin{aligned}\overline{P}_0\overline{\sigma}_x &= \overline{Q}_0\overline{\varepsilon}_x + \overline{Q}_1\overline{\varepsilon}_y\\ \overline{P}_0\overline{\sigma}_y &= \overline{Q}_1\overline{\varepsilon}_x + \overline{Q}_0\overline{\varepsilon}_y\\ \overline{P}'\overline{\tau}_{xy} &= \overline{Q}'\overline{\varepsilon}_{xy}\end{aligned} \tag{5}$$

Then

$$\begin{aligned}\varepsilon_x &= \frac{\partial u}{\partial x} = -z\frac{\partial^2 w}{\partial x^2}\\ \varepsilon_y &= \frac{\partial v}{\partial y} = -z\frac{\partial^2 w}{\partial y^2}\\ \gamma_{xy} &= \frac{\partial u}{\partial y} + \frac{\partial v}{\partial x} = -2z\frac{\partial^2 w}{\partial x\partial y}.\end{aligned} \tag{6}$$

According to the thin plate theory, moment and torque of the hard membrane are defined as follows.

$$\begin{aligned}M_x &= \int_{-h/2}^{h/2} z\sigma_x dz\\ M_y &= \int_{-h/2}^{h/2} z\sigma_y dz\end{aligned} \tag{7}$$

$$M_{xy} = \int_{-h/2}^{h/2} z\tau_{xy}dz = M_{yx} = \int_{-h/2}^{h/2} z\tau_{yx}dz \tag{8}$$

Laplace transform is performed on (7) and (8), and then they are multiplied by $\overline{P}_0, \overline{P}'$.

$$\begin{aligned}\overline{P}_0\left(\overline{M}_x\right) &= \int_{-h/2}^{h/2} z\overline{P}_0\left(\overline{\sigma}_x\right)dz\\ \overline{P}_0\left(\overline{M}_y\right) &= \int_{-h/2}^{h/2} z\overline{P}_0\left(\overline{\sigma}_y\right)dz\\ \overline{P}'\left(\overline{M}_{xy}\right) &= \int_{-h/2}^{h/2} z\overline{P}'\left(\overline{\tau}_{xy}\right)dz\end{aligned} \tag{9}$$

Substituting (5) and (6) into (9) yields the following.

$$\begin{aligned}\overline{P}_0\left(\overline{M}_x\right) &= -\int_{-h/2}^{h/2} z^2\left(\overline{Q}_0\frac{\partial^2\overline{w}}{\partial x^2} + \overline{Q}_1\frac{\partial^2\overline{w}}{\partial y^2}\right)dz\\ \overline{P}_0\left(\overline{M}_y\right) &= -\int_{-h/2}^{h/2} z^2\left(\overline{Q}_1\frac{\partial^2\overline{w}}{\partial x^2} + \overline{Q}_0\frac{\partial^2\overline{w}}{\partial y^2}\right)dz\\ \overline{P}'\left(\overline{M}_{xy}\right) = \overline{P}'\left(\overline{M}_{yx}\right) &= -\int_{-h/2}^{h/2} z^2\overline{Q}'\left(\frac{\partial^2\overline{w}}{\partial x\partial y}\right)dz\end{aligned} \tag{10}$$

The speed of the moving hard membrane in the z direction is as follows.

$$\overline{v}(t) = \frac{dw}{dt} = \frac{\partial w}{\partial t} + v\frac{\partial w}{\partial x} \tag{11}$$

Acceleration in the z direction is written as follows.

$$\begin{aligned}\overline{a} &= \frac{d\overline{v}}{dt}\\ &= \frac{\partial\left(\partial w/\partial t + v\left(\partial w/\partial x\right)\right)}{\partial t}\\ &\quad + v\frac{\partial\left(\partial w/\partial t + v\left(\partial w/\partial x\right)\right)}{\partial x}\\ &= \frac{\partial^2 w}{\partial t^2} + 2v\frac{\partial^2 w}{\partial x\partial t} + v^2\frac{\partial^2 w}{\partial x^2}\end{aligned} \tag{12}$$

The partial differential equation of the hard membrane is obtained according to the d'Alembert principle.

$$\begin{aligned}&\frac{\partial^2 M_x}{\partial x^2} + 2\frac{\partial^2 M_{xy}}{\partial x\partial y} + \frac{\partial^2 M_y}{\partial y^2}\\ &\quad - \rho h\left(\frac{\partial^2 w}{\partial t^2} + 2v\frac{\partial^2 w}{\partial x\partial t} + v^2\frac{\partial^2 w}{\partial x^2}\right) = 0\end{aligned} \tag{13}$$

Performing a Lagrangian transformation on (13), then multiplying it by $\overline{P}_0\overline{P}'$, the following equation is obtained.

$$\begin{aligned}&\overline{P}_0\overline{P}'\left(\frac{\partial^2\overline{M}_x}{\partial x^2}\right) + 2\overline{P}_0\overline{P}'\left(\frac{\partial^2\overline{M}_{xy}}{\partial x\partial y}\right)\\ &\quad + \overline{P}_0\overline{P}'\left(\frac{\partial^2\overline{M}_y}{\partial y^2}\right) - \rho h\overline{P}_0\overline{P}'\left(s_1^2\overline{w}\right.\\ &\quad \left. + 2vs_1\frac{\partial\overline{w}}{\partial x} + v^2\frac{\partial^2\overline{w}}{\partial x^2}\right) = 0\end{aligned} \tag{14}$$

Equation (14) is changed into the following.

$$\begin{aligned}&\overline{P}'\left(\frac{\partial^2\left[\overline{P}_0\left(\overline{M}_x\right)\right]}{\partial x^2}\right) + 2\overline{P}_0\left(\frac{\partial^2\left[\overline{P}'\left(\overline{M}_{xy}\right)\right]}{\partial x\partial y}\right)\\ &\quad + \overline{P}'\left(\frac{\partial^2\left[\overline{P}_0\left(\overline{M}_y\right)\right]}{\partial y^2}\right)\\ &\quad - \rho h\overline{P}_0\overline{P}'\left(s_1^2\overline{w} + 2vs_1\frac{\partial\overline{w}}{\partial x} + v^2\frac{\partial^2\overline{w}}{\partial x^2}\right) = 0\end{aligned} \tag{15}$$

Substituting (10) into (15), the differential equation of a hard printing membrane in the Lagrangian domain is obtained.

$$\begin{aligned}&\frac{h^3}{12}\overline{P}'\overline{Q}_0\nabla^4\overline{w} + \rho h\overline{P}_0\overline{P}'\left(s_1^2\overline{w} + 2vs_1\frac{\partial\overline{w}}{\partial x} + v^2\frac{\partial^2\overline{w}}{\partial x^2}\right)\\ &\quad = 0\end{aligned} \tag{16}$$

Assuming that the shape distortion of the hard printing membrane satisfies the Kelvin-Voigt model, then we obtain the following.

$$\begin{aligned} \overline{P}' &= 1, \\ \overline{Q}' &= 2G + 2\eta s_1 \\ \overline{P}'' &= 1, \\ \overline{Q}'' &= 3K \end{aligned} \tag{17}$$

Substituting (17) into (16) and then performing inverse Lagrangian transformation, the differential equation of the moving hard membrane in the time domain that satisfies the Kelvin-Voigt model is obtained:

$$\begin{aligned} &\frac{h^3}{12}\left(A_3 + A_4\frac{\partial}{\partial t} + A_5\frac{\partial^2}{\partial t^2}\right)\nabla^4 w_I \\ &\quad + \rho h\left(A_1 + A_2\frac{\partial}{\partial t}\right)\left(\frac{\partial^2 w_I}{\partial t^2} + 2v\frac{\partial^2 w_I}{\partial t \partial x} + v^2\frac{\partial^2 w_I}{\partial x^2}\right) \\ &\quad = 0 \end{aligned} \tag{18}$$

where $A_1 = 3K + 4G$, $A_2 = 4\eta$, $A_3 = 2G(6K + 2G)$, $A_4 = 8G\eta + 12K\eta$, $A_5 = 4\eta^2$, $G = E/2(1 + \mu)$, $K = E/3(1 - 2\mu)$, μ denotes the Poisson's ratio of the hard membrane, $\nabla^4 w_I = \partial^4 w_I/\partial x^4 + 2(\partial^4 w_I/\partial x^2 \partial y^2) + \partial^4 w_I/\partial y^4$.

The discontinuity of the hard membrane is caused by the scratches. Θ is additional angle caused by scratches. The continuous conditions of the scratch [20–22] are (19a)-(19d).

The deflection is as follows.

$$w_I\left(x_I^-, y, t\right) = w_{I+1}\left(x_I^+, y, t\right) \tag{19a}$$

The bending moment is as follows.

$$M_{Ix}\left(x_I^-, y, t\right) = M_{(I+1)x}\left(x_I^+, y, t\right) \tag{19b}$$

The equivalent shear is as follows.

$$V_{Ix}\left(x_I^-, y, t\right) = V_{(I+1)x}\left(x_I^+, y, t\right) \tag{19c}$$

The angle is

$$w_{I,x}\left(x_I^-, y, t\right) + \Theta - w_{I+1,x}\left(x_I^+, y, t\right) = 0 \tag{19d}$$

where $V_{Ix} = Q_{Ix} + M_{Ixy,y}$.

Performing a Lagrangian transformation on (18), then multiplying it by $\overline{P}_0$, $\overline{P}_0\overline{P}'$, the following equations are obtained:

$$\overline{w}_I\left(x_I^-, y\right) = \overline{w}_{I+1}\left(x_I^+, y\right) \tag{20a}$$

$$\overline{P}_0\left(\overline{M}_{Ix}\left(x_I^-, y\right)\right) = \overline{P}_0\left(\overline{M}_{(I+1)x}\left(x_I^+, y\right)\right) \tag{20b}$$

$$\begin{aligned} &\overline{P}_0\overline{P}'\left(\overline{Q}_{Ix}\left(x_I^-, y\right)\right) + \overline{P}_0\overline{P}'\left(\overline{M}_{Ixy,y}\left(x_I^-, y\right)\right) \\ &\quad = \overline{P}_0\overline{P}'\left(\overline{Q}_{(I+1)x}\left(x_I^+, y\right)\right) \\ &\quad + \overline{P}_0\overline{P}'\left(\overline{M}_{(I+1)xy,y}\left(x_I^+, y\right)\right) \end{aligned} \tag{20c}$$

$$\overline{w}_{I,x}\left(x_I^-, y\right) + \overline{\Theta} - \overline{w}_{I+1,x}\left(x_I^+, y\right) = 0 \tag{20d}$$

where

$$\begin{aligned} &3\overline{Q}'\overline{Q}''\left(2\overline{P}'\overline{Q}'' + \overline{P}''\overline{Q}'\right)\overline{\Theta} \\ &= 12\left[\left(2\overline{P}'\overline{Q}'' + \overline{P}''\overline{Q}'\right)^2 - \left(\overline{P}'\overline{Q}'' - \overline{P}''\overline{Q}'\right)^2\right]\alpha_{bb}\overline{\sigma}_b. \end{aligned} \tag{21}$$

Performing a Lagrangian transformation on σ_b and multiplying it by $\overline{P}_0$, we get the following.

$$\begin{aligned} &2\overline{P}'\left(\overline{P}'\overline{Q}'' + 2\overline{Q}'\overline{P}''\right)\overline{\sigma}_b \\ &\quad = -h\overline{Q}'\left[\left(2\overline{P}'\overline{Q}'' + \overline{P}''\overline{Q}'\right)\frac{\partial^2\overline{w}_I}{\partial x^2}\right. \\ &\quad \left. + \left(\overline{P}'\overline{Q}'' - \overline{P}''\overline{Q}'\right)\frac{\partial^2\overline{w}_I}{\partial y^2}\right] \end{aligned} \tag{22}$$

The scratch characteristic coefficient is denoted as α_{bb}

$$\alpha_{bb} = \int_0^{S_c} {g_b}^2 d\varsigma \tag{23}$$

where $S_c = h_c/h$, and scratch depth function g_b is defined as follows.

$$\begin{aligned} &g_b \\ &\quad = \varsigma^{1/2}\left(1.99 - 2.47\varsigma + 12.97\varsigma^2 - 23.17\varsigma^3 + 24.80\varsigma^4\right) \end{aligned} \tag{24}$$

The viscoelastic membrane body changes to an elastic one, and the shape distortion satisfies the Kelvin-Voigt model; then we obtain

$$\begin{aligned} &\left(A_6 + A_7\frac{\partial}{\partial t}\right)\Theta = -6h\alpha_{bb}\left[\left(A_6 + A_7\frac{\partial}{\partial t}\right)\frac{\partial^2 w_I}{\partial x^2}\right. \\ &\quad \left. + \left(A_8 - A_7\frac{\partial}{\partial t}\right)\frac{\partial^2 w_I}{\partial y^2}\right] \end{aligned} \tag{25}$$

where $A_6 = 6K + 2G$, $A_7 = 2\eta$, $A_8 = 3K - 2G$.

The dimensionless quantities are expressed as follows.

$$\begin{aligned} \xi &= \frac{x}{a}, \\ \psi &= \frac{y}{b}, \\ \overline{W}_I &= \frac{w_I}{a}, \\ \lambda &= \frac{a}{b}, \\ r &= \frac{h}{a}, \\ \tau &= \frac{th}{a^2}\sqrt{\frac{E}{12\rho\left(1 - \mu^2\right)}}, \end{aligned}$$

$$c = \frac{a}{h}\sqrt{\frac{12\rho\left(1-\mu^2\right)}{E}}v,$$

$$H = \frac{h}{a^2}\sqrt{\frac{E}{12\rho\left(1-\mu^2\right)}}\frac{\eta}{E} \tag{26}$$

The dimensionless governing equations of the moving hard membrane can be obtained as follows:

$$\begin{aligned}&\left[1+\frac{4\left(2-\mu\right)\left(1+\mu\right)}{3}H\frac{\partial}{\partial\tau}\right.\\&\left.+\frac{4\left(1-2\mu\right)\left(1+\mu\right)^2}{3}H^2\frac{\partial^2}{\partial\tau^2}\right]\nabla^4\overline{W}_I+\left[1\right.\\&\left.+\frac{4\left(1-2\mu\right)\left(1+\mu\right)}{3\left(1-\mu\right)}H\frac{\partial}{\partial\tau}\right]\left(\frac{\partial^2\overline{W}_I}{\partial\tau^2}+2c\frac{\partial^2\overline{W}_I}{\partial\xi\partial\tau}\right.\\&\left.+c^2\frac{\partial^2\overline{W}_I}{\partial\xi^2}\right)=0\end{aligned} \tag{27}$$

where H represents dimensionless delay time, c represents the dimensionless speed, τ is dimensionless time, $\nabla^4\overline{W}_I = \partial^4\overline{W}_I/\partial\xi^4 + 2\lambda^2(\partial^4\overline{W}_I/\partial\xi^2\partial\psi^2) + \lambda^4(\partial^4\overline{W}_I/\partial\psi^4)$.

The dimensionless continuous conditions of the scratch are

$$\begin{aligned}&\overline{W}_I\left(\xi_I^-,\psi,\tau\right)=\overline{W}_{I+1}\left(\xi_I^+,\psi,\tau\right)\\&B_1\frac{\partial^2\overline{W}_I\left(\xi_I^-,\psi,\tau\right)}{\partial\xi^2}+B_2\lambda^2\frac{\partial^2\overline{W}_I\left(\xi_I^-,\psi,\tau\right)}{\partial\psi^2}\\&\quad=B_1\frac{\partial^2\overline{W}_{I+1}\left(\xi_I^+,\psi,\tau\right)}{\partial\xi^2}+B_2\lambda^2\frac{\partial^2\overline{W}_{I+1}\left(\xi_I^+,\psi,\tau\right)}{\partial\psi^2}\\&B_1\frac{\partial^3\overline{W}_I\left(\xi_I^-,\psi,\tau\right)}{\partial\xi^3}+B_3\lambda^2\frac{\partial^3\overline{W}_I\left(\xi_I^-,\psi,\tau\right)}{\partial\xi\partial\psi^2}\\&\quad=B_1\frac{\partial^3\overline{W}_{I+1}\left(\xi_I^+,\psi,\tau\right)}{\partial\xi^3}+B_3\lambda^2\frac{\partial^3\overline{W}_{I+1}\left(\xi_I^+,\psi,\tau\right)}{\partial\xi\partial\psi^2}\\&B_1\left(\frac{\partial\overline{W}_I\left(\xi_I^-,\psi,\tau\right)}{\partial\xi}-\frac{\partial\overline{W}_{I+1}\left(\xi_I^+,\psi,\tau\right)}{\partial\xi}\right)\\&\quad=-6r\alpha_{bb}\left(B_1\frac{\partial^2\overline{W}_I\left(\xi_I^-,\psi,\tau\right)}{\partial\xi^2}\right.\\&\left.\quad+B_2\lambda^2\frac{\partial^2\overline{W}_I\left(\xi_I^-,\psi,\tau\right)}{\partial\psi^2}\right)\end{aligned} \tag{28}$$

where $B_1 = 1+(2/3)(1-2\mu)(1+\mu)H(\partial/\partial\tau)$, $B_2 = \mu-(2/3)(1-2\mu)(1+\mu)H(\partial/\partial\tau)$, $B_3 = (2-\mu)+2(1-2\mu)(1+\mu)H(\partial/\partial\tau)$.

Supposing the solution of (27) is $\overline{W}_I(\xi,\psi,\tau) = W_I(\xi,\psi)e^{j\omega\tau}$, the vibration differential equation of the moving hard membrane that satisfies the Kelvin-Voigt model is expressed as

$$D_1\nabla^4W_I+D_2\left(-\omega^2W_I+2cj\omega\frac{\partial W_I}{\partial\xi}+c^2\frac{\partial^2W_I}{\partial\xi^2}\right)=0 \tag{29}$$

where $D_1 = 1-(4(1-2\mu)(1+\mu)^2/3)H^2\omega^2+(4(2-\mu)(1+\mu)/3)H\omega j$, $D_2 = 1+(4(1-2\mu)(1+\mu)/3(1-\mu))H\omega j$, $j=\sqrt{-1}$, ω is the frequency of a hard membrane.

Substituting $\overline{W}_I(\xi,\psi,\tau) = W_I(\xi,\psi)e^{j\omega\tau}$ into (28) yields

$$\begin{aligned}&W_I\left(\xi_I^-,\psi\right)=W_{I+1}\left(\xi_I^+,\psi\right)\\&D_3\frac{\partial^2W_I\left(\xi_I^-,\psi\right)}{\partial\xi^2}+D_4\lambda^2\frac{\partial^2W_{I+1}\left(\xi_I^-,\psi\right)}{\partial\psi^2}\\&\quad=D_3\frac{\partial^2W_{I+1}\left(\xi_I^+,\psi\right)}{\partial\xi^2}+D_4\lambda^2\frac{\partial^2W_{I+1}\left(\xi_I^+,\psi\right)}{\partial\psi^2}\\&D_3\frac{\partial^3W_I\left(\xi_I^-,\psi\right)}{\partial\xi^3}+D_5\lambda^2\frac{\partial^3W_I\left(\xi_I^-,\psi\right)}{\partial\xi\partial\psi^2}\\&\quad=D_3\frac{\partial^3W_{I+1}\left(\xi_I^+,\psi\right)}{\partial\xi^3}+D_5\lambda^2\frac{\partial^3W_{I+1}\left(\xi_I^+,\psi\right)}{\partial\xi\partial\psi^2}\\&D_3\left(\frac{\partial W_I\left(\xi_I^-,\psi\right)}{\partial\xi}-\frac{\partial W_{I+1}\left(\xi_I^+,\psi\right)}{\partial\xi}\right)\\&\quad=-6r\alpha_{bb}\left(D_3\frac{\partial^2W_I\left(\xi_I^-,\psi\right)}{\partial\xi^2}+D_4\lambda^2\frac{\partial^2W_I\left(\xi_I^-,\psi\right)}{\partial\psi^2}\right)\end{aligned} \tag{30}$$

where $D_3 = 1+(2/3)(1-2\mu)(1+\mu)Hj\omega$, $D_5 = (2-\mu)+2(1-2\mu)(1+\mu)Hj\omega$, $D_4 = \mu-(2/3)(1-2\mu)(1+\mu)Hj\omega$.

The boundary conditions of a moving viscoelastic hard membrane are as follows.

$$\begin{aligned}&\xi=0,1:\quad W\left(\xi,\psi\right)=\frac{\partial W}{\partial\xi}=0\\&\psi=0,1:\quad W\left(\xi,\psi\right)=\frac{\partial^2W}{\partial\psi^2}=0\end{aligned} \tag{31}$$

3. Solving Equation

Equation (28) is discretized by differential quadrature method [23].

$$\frac{4\left(1-2\mu\right)\left(1+\mu\right)}{3\left(1-\mu\right)}Hj^3W_{ij}\omega^3+\left[\frac{4\left(1-2\mu\right)\left(1+\mu\right)^2}{3}\right.$$

$$\cdot H^2 \mathrm{j}^2 \left(\sum_{k=1}^{N} A_{ik}{}^{(4)} W_{kj} + 2\lambda^2 \sum_{m=1}^{N} B_{jm}{}^{(2)} \sum_{k=1}^{N} A_{ik}{}^{(2)} W_{km} + \lambda^4 \sum_{k=1}^{N} B_{jk}{}^{(4)} W_{ik} \right) + \frac{4(1-2\mu)(1+\mu)}{3(1-\mu)} 2cH\mathrm{j}^2 \sum_{k=1}^{N} A_{ik} W_{kj} + \mathrm{j}^2 W_{ij} \Bigg] \omega^2 + \Bigg[\frac{4(2-\mu)(1+\mu)}{3} H\mathrm{j} \left(\sum_{k=1}^{N} A_{ik}{}^{(4)} W_{kj} + 2\lambda^2 \sum_{m=1}^{N} B_{jm}{}^{(2)} \sum_{k=1}^{N} A_{ik}{}^{(2)} W_{km} + \lambda^4 \sum_{k=1}^{N} B_{jk}{}^{(4)} W_{ik} \right) + \frac{4(1-2\mu)(1+\mu)}{3(1-\mu)} Hjc^2 \sum_{k=1}^{N} A_{ik}{}^{(2)} W_{kj} + 2cj \sum_{k=1}^{N} A_{ik} W_{kj} \Bigg] \omega + \sum_{k=1}^{N} A_{ik}{}^{(4)} W_{kj} + 2\lambda^2 \sum_{m=1}^{N} B_{jm}{}^{(2)} \cdot \sum_{k=1}^{N} A_{ik}{}^{(2)} W_{km} + \lambda^4 \sum_{k=1}^{N} B_{jk}{}^{(4)} W_{ik} + c^2 \sum_{k=1}^{N} A_{ik}{}^{(2)} W_{kj} = 0 \tag{32}$$

Scratch continuous conditions are discretized by differential quadrature method

$$W_{cj} - W_{cj} = 0 \quad (j = 1, 2, \ldots, N) \tag{33}$$

$$D_3 \sum_{k=1}^{N} A_{c+2,k}{}^{(2)} W_{kj} + D_4 \lambda^2 \sum_{m=1}^{N} A_{c+2,m}{}^{(2)} W_{km} = D_3 \sum_{k=1}^{N} A_{c+2,k}{}^{(2)} W_{kj} + D_4 \lambda^2 \sum_{m=1}^{N} A_{c+2,m}{}^{(2)} W_{km} \tag{34a}$$

$$D_3 \sum_{k=1}^{N} A_{c+3,k}{}^{(3)} W_{kj} + D_5 \lambda^2 \sum_{k=1}^{N} A_{c+3,k}{}^{(1)} \sum_{m=1}^{N} A_{c+3,m}{}^{(2)} W_{km} = D_3 \sum_{k=1}^{N} A_{c+3,k}{}^{(3)} W_{kj} + D_5 \lambda^2 \sum_{k=1}^{N} A_{c+3,k}{}^{(1)} \sum_{m=1}^{N} A_{c+3,m}{}^{(2)} W_{km} \tag{34b}$$

$$D_3 \sum_{k=1}^{N} A_{c+1,k}{}^{(1)} W_{kj} + D_3 \sum_{k=1}^{N} A_{c+1,k}{}^{(1)} W_{kj} + 6r\alpha_{bb} \left(D_3 \sum_{k=1}^{N} A_{c+1,k}{}^{(2)} W_{kj} + D_4 \lambda^2 \sum_{k=1}^{N} A_{c+1,k}{}^{(2)} W_{kj} \right) = 0 \tag{34c}$$

The numbers of discrete points in the x and y directions are equal. The discrete forms of the node are as follows.

$$\begin{aligned} &\xi_1 = 0, \\ &\xi_N = 1, \\ &\xi_i = \frac{1}{2}\left[1 - \cos\left(\frac{2i-3}{2N-4}\pi\right)\right] \quad (i = 2, 3, \ldots, N-1) \\ &\psi_1 = 0, \\ &\psi_N = 1, \\ &\psi_i = \frac{1}{2}\left[1 - \cos\left(\frac{2i-3}{2N-4}\pi\right)\right] \quad (i = 2, 3, \ldots, N-1) \end{aligned} \tag{35a}$$

$$\begin{aligned} &\xi_1 = 0, \\ &\xi_2 = \delta, \\ &\xi_{N-1} = 1 - \delta, \\ &\xi_N = 1, \\ &\xi_i = \frac{1}{2}\left[1 - \cos\left(\frac{i-2}{N-3}\pi\right)\right] \quad (i = 3, 4, \ldots, N-2) \\ &\psi_1 = 0, \\ &\psi_N = 1, \\ &\psi_i = \frac{1}{2}\left[1 - \cos\left(\frac{2i-3}{2N-4}\pi\right)\right] \quad (i = 2, 3, \ldots, N-1) \end{aligned} \tag{35b}$$

Then the discrete forms of boundary conditions in equation (31) are as follows.

$$W_{1j} = W_{Nj} = W_{i1} = W_{iN} = 0 \quad (i, j = 1, 2, \ldots, N)$$

$$\sum_{k=1}^{N} A_{ik}{}^{(2)} W_{kj} = 0 \quad (i = 1, N \ j = 1, 2, \ldots, N) \tag{36}$$

$$\sum_{k=1}^{N} B_{jk}{}^{(2)} W_{ik} = 0 \quad (j = 1, N \ i = 1, 2, \ldots, N)$$

Table 1: Comparison between the natural frequencies of a moving viscoelastic hard membrane and [12](c=2, H=10^{-5}).

aspect ratio	This paper			Reference [12]		
	ω_1	ω_2	ω_3	ω_1	ω_2	ω_3
λ=1	27.490	53.580	68.090	27.487	53.576	68.091
λ=0.8	24.820	40.520	65.270	24.818	40.519	65.267

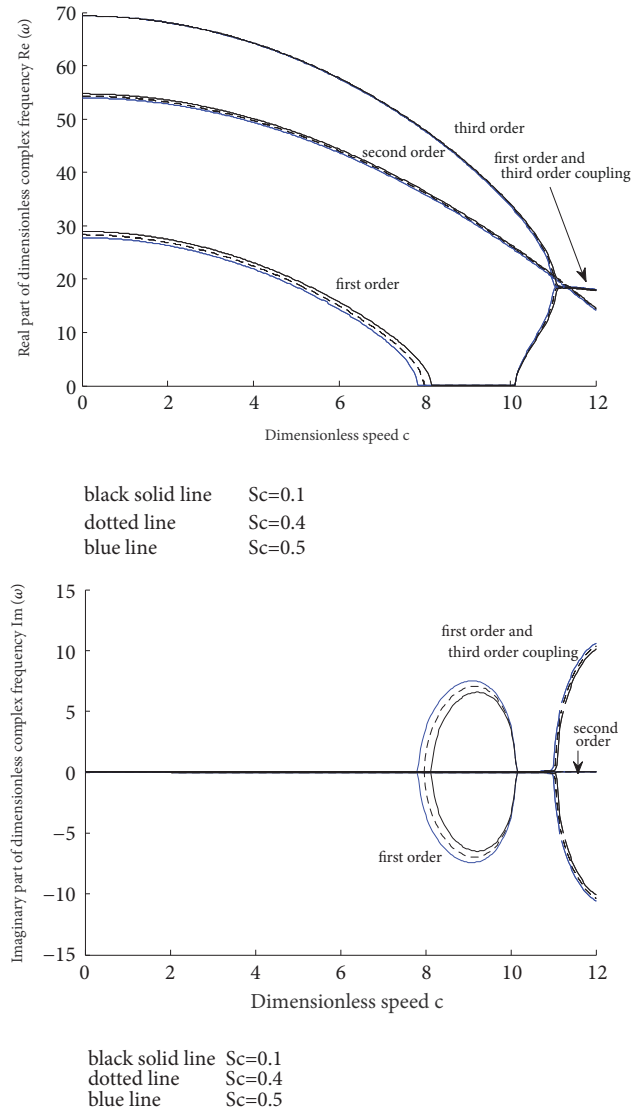

Figure 2: The relationship of complex frequencies and velocity under different scratch depths ($H = 10^{-6}, \lambda = 1, \xi_c = 0.5$).

Combine (36) with (32), (33), (34a), (34b) and (34c):

$$\left(\omega^3 \boldsymbol{Q} + \omega^2 \boldsymbol{R} + \omega \boldsymbol{G} + \boldsymbol{K}\right)\left\{W_{kj}\right\} = \{\boldsymbol{0}\} \tag{37}$$

with $\boldsymbol{Q}$, $\boldsymbol{R}$, $\boldsymbol{G}$, $\boldsymbol{K}$ including scratch position ξ_c, scratch depth S_c, hard membrane thickness ratio r, aspect ratio λ, delay time H, and moving speed c.

The characteristic equation of the hard membrane with a scratch is expressed as follows.

$$\left|\omega^3 \boldsymbol{Q} + \omega^2 \boldsymbol{R} + \omega \boldsymbol{G} + \boldsymbol{K}\right| = 0 \tag{38}$$

4. Numerical Results

When delay time H=10^{-5}, moving speed c = 2, scratch depth S_c = 0, the problem degenerates into a vibration problem of a moving viscoelastic hard membrane without scratches. The vibration natural frequency of the nonscratched moving viscoelastic hard membrane is solved and then compared with [12] as shown in Table 1.

As a result, the natural frequency of a moving viscoelastic hard membrane without scratches is consistent with the literature solution.

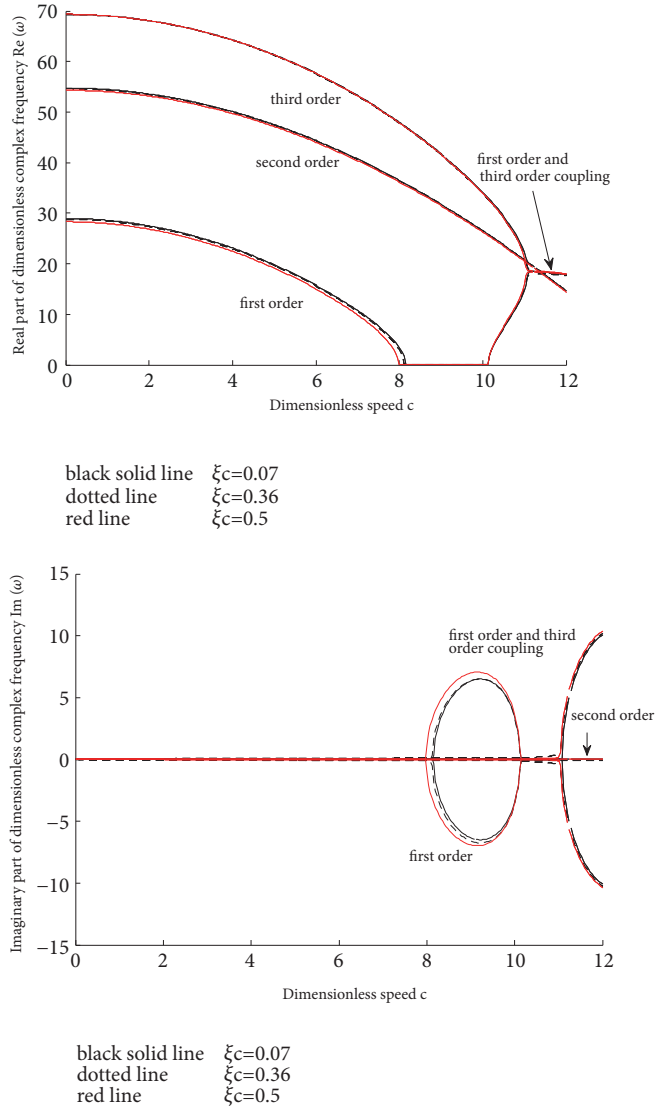

Figure 3: The relationship of complex frequencies and velocity under different scratch position ($H = 10^{-6}, \lambda = 1, S_c = 0.4$).

4.1. The Effects of Scratch Depth on Stability. Figure 3 shows the relationship between the complex frequency of a hard membrane and the speed with the different scratch depths; aspect ratio $\lambda = 1$, delay time $H = 10^{-6}$, scratch position is 0.5, and the scratch depth is 0.1, 0.4, 0.5, separately. When scratch depth $S_c = 0.5$, $0 \leq c < 7.8$, the imaginary parts of the first three modes are zero, and the real parts are decreased. When the speed c=7.8, the first-order frequency $\mathrm{Re}(\omega) = 0$, the imaginary part has both positive and negative values, and the membrane is divergent and unstable. When $c = 10.16$, the membrane becomes stable again. When c=11, the first and third modes are coupled chatter. Comparing the three curves when $S_c = 0.1$,0.4, 0.5, it can be seen that the variation laws of the real part and the imaginary part of the frequencies containing different scratch depths are almost the same. When the scratch depth is deeper, the critical divergence velocity and the critical velocity of coupled chatter are smaller.

4.2. The Effects of Scratch Position on Stability. Figure 3 shows the relationship between the complex frequencies and membrane speed with the different scratch position; the aspect ratio $\lambda = 1$, the delay time H is 10^{-6}, the scratch depth S_c is 0.4, and the scratch position ξ_c is 0.07, 0.36, 0.5, respectively. When $\xi_c = 0.07$, the speed $0 \leq c < 8.16$, the imaginary parts of the first three modes are zero, and the real parts are decreased with the increase of the speed. When the speed c=8.16, the first-order mode is divergence instability. When the speed c=10.12, the membrane becomes stable again. When c=11.08, the first and third modes are coupled chatter. It can be seen from Figure 3 that the scratch depth is kept constant; the closer the scratch position is to the middle portion, the lower the critical speed is when hard membrane shows the divergence instability and coupled chatter instability.

4.3. The Effects of Scratch Depth and Scratch Position on Stability. Figures 4, 5, and 6 show the relationship between

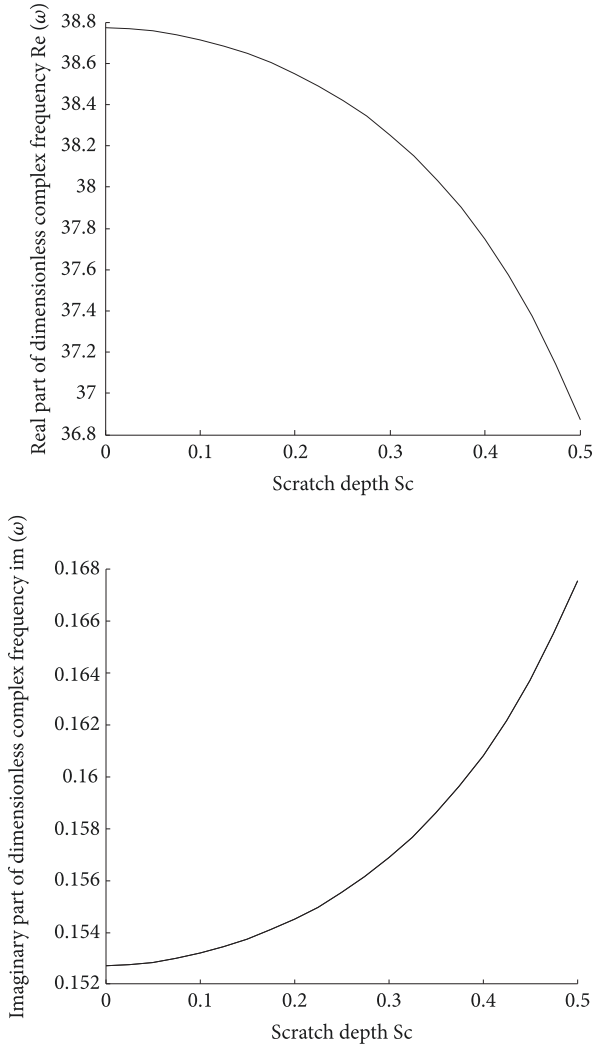

Figure 4: The relationship of first-order complex frequencies and scratch depth ($H = 10^{-4}, \lambda = 1.5, c = 1, \xi_c = 0.5$).

the complex frequencies of the hard membrane and the scratch depth when the scratch depth is gradually increased, and the parameters are $H = 10^{-4}, \lambda = 1.5$, $c = 1$, $\xi_c = 0.5$. It is noted that when the scratch depth gradually increases, the real part of complex frequency decreases, the imaginary part increases, and change laws of the first-order, second-order, and third-order modes are the same. As a result, the occurrence of scratches can lead to the decrease of the membrane stiffness, and the stiffness is reduced with the increase of the scratch depth.

Figure 7 shows the relationship between the complex frequency of the hard membrane and the scratch position, when $H = 10^{-4}$, $\lambda = 1.5$, $c = 1$, $S_c = 0.4$. It can be noted that when the scratch position changes from left to right, the real part of the complex frequency firstly decreases and then increases, and the imaginary part firstly decreases, then increases, and lastly decreases. The real part and imaginary part of the complex frequency are equal when the scratch positions are $\xi_c = 1$ and $\xi_c = 0$. The real part of complex frequency is the smallest when the scratch position is in the middle.

4.4. Coupling Effect of Speed and Scratch Depth on Membrane Vibration. Tables 2 and 3 show the frequency ratio ($\mathrm{Re}\,\omega_c/\mathrm{Re}\,\omega$) caused by the scratch depth under different speeds, and the frequency ratio ($\mathrm{Re}\,\omega_v/\mathrm{Re}\,\omega$) caused by the speed under different scratch depths. It can be seen from Table 2 that the frequency is decreasing with the increase in the scratch depth, and the frequency reduction caused by scratches becomes faster as the speed increases. It can be seen from Table 3 that the frequency is decreasing along with the speed increasing, and the frequency reduction caused by the speed becomes faster as the scratch depth expands. It is noted that the coupling of speed and scratch depth affects the hard membrane frequency.

4.5. Numeral Calculations. As can be seen from Figure 2, the hard membrane undergoes divergence instability when

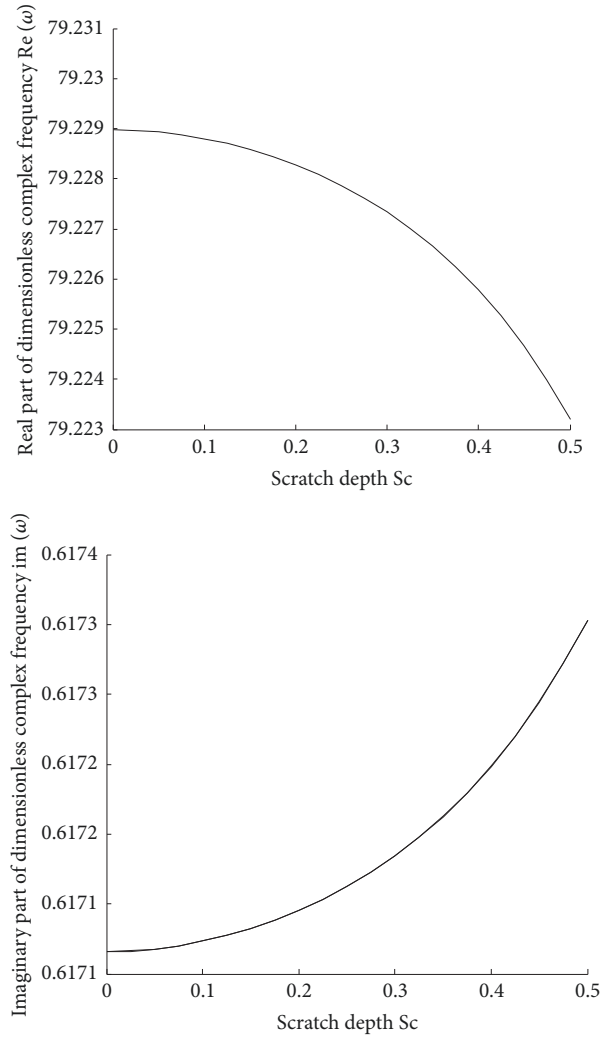

Figure 5: The relationship of second-order complex frequencies and scratch depth ($H = 10^{-4}, \lambda = 1.5, c = 1, \xi_c = 0.5$).

Table 2: Frequency ratios versus the scratch depth.

Speed v	Initial Re ω	Frequency ratio Re ω_c/Re ω (%) Scratch depth S_c				
		0.1	0.2	0.3	0.4	0.5
0	39.09	99.86	99.43	98.67	97.38	95.13
2	37.80	99.85	99.42	98.64	97.31	95.00
4	33.98	99.84	99.37	98.52	97.08	94.56
6	27.69	99.81	99.25	98.24	96.52	93.48
8	19.03	99.73	98.92	97.45	94.93	90.39

the dimensionless speed c=7.8. The relationship between the dimensionless speed and the actual moving speed [11] is as follows.

$$v = \frac{ch}{a\sqrt{12\rho\left(1-\mu^2\right)/E}} \tag{39}$$

The basic parameters of a precision coating hard membrane are shown in Table 4. The hard membrane undergoes divergence instability when the actual printing speed is v=23.2 m/s; that is, the membrane is stable when v<23.2 m/s.

5. Conclusions

The transverse vibration and stability of a moving viscoelastic hard membrane containing scratches are investigated. The conclusions are below:

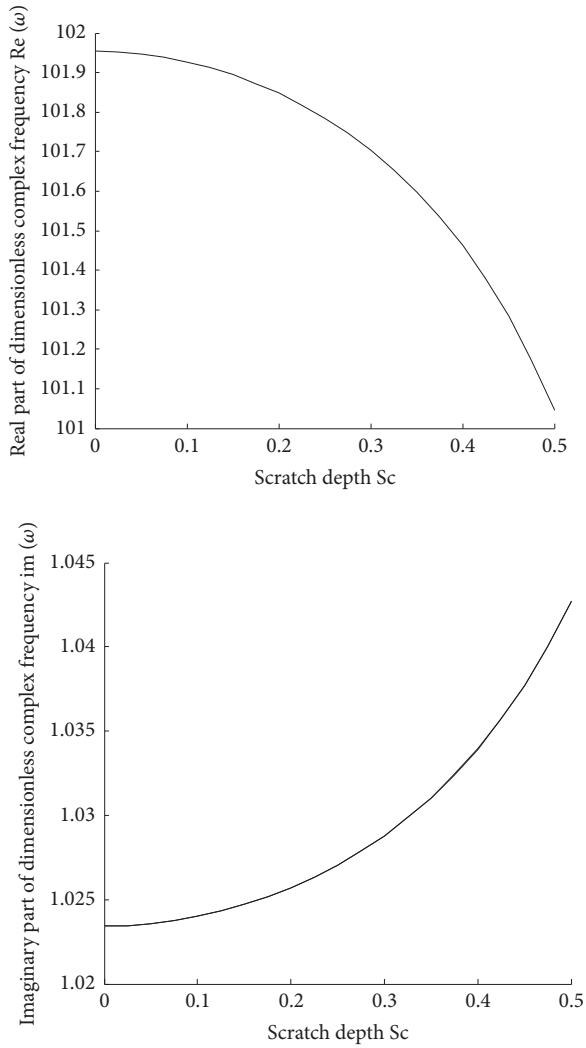

Figure 6: The relationship of third-order complex frequencies and scratch depth ($H = 10^{-4}, \lambda = 1.5, c = 1, \xi_c = 0.5$).

Table 3: Frequency ratios versus the axial velocity.

Scratch depth S_c	Initial Re ω	Frequency ratio Re ω_v/Re ω (%) Speed v			
		2	4	6	8
0.0	39.09	96.71	86.93	70.84	48.68
0.1	39.04	96.71	86.91	70.81	48.62
0.2	38.87	96.70	86.87	70.72	48.43
0.3	38.57	96.68	86.80	70.54	48.08
0.4	38.07	96.65	86.67	70.22	47.46
0.5	37.19	96.59	86.42	69.62	46.26

(1) The critical speeds of the flutter instability and divergence instability are decreasing with the increase of the scratch depth.

(2) Changes in the scratch position will affect the unstable form of the hard membrane. When the moving speed is increasing, the closer the scratch position is to the middle, the more easily the hard membrane experiences flutter instability and divergence instability.

(3) The coupling of speed and scratch depth affects the hard membrane frequency. The frequency reduction caused

Table 4: The basic parameters of the precision coating hard membrane.

parameters	parameters	values
a	hard membrane width	$530mm$
h	hard membrane thickness	$1.2mm$
ρ	density	$333kg/m^3$
μ	Poisson's ratio	0.3
E	elastic modulus	$6.26G/Pa$

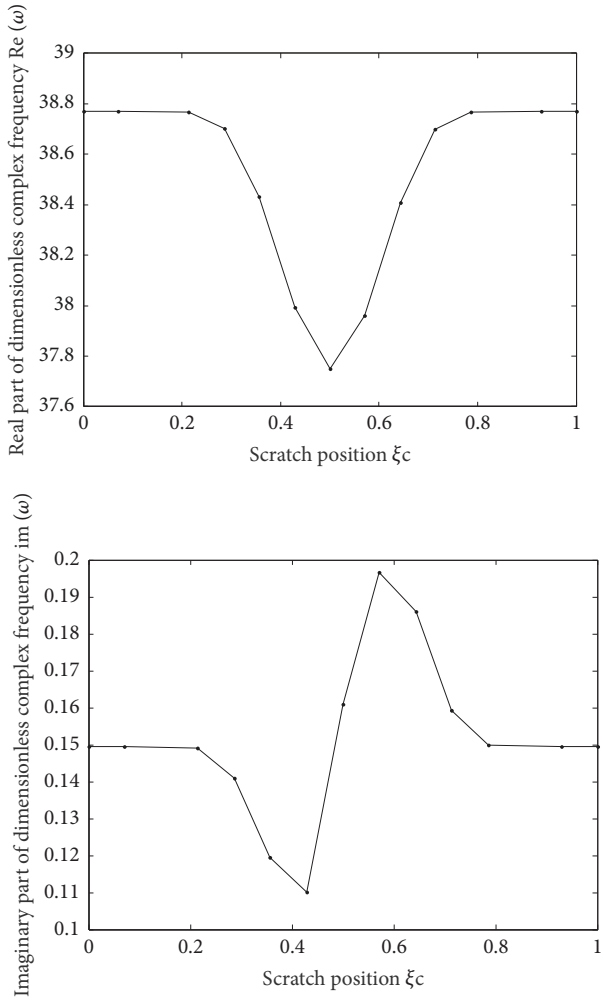

Figure 7: The first-order complex frequencies versus scratch position ($H = 10^{-4}, \lambda = 1.5, c = 1, S_c = 0.4$).

by scratches becomes faster as the speed increases, and the frequency reduction caused by the speed becomes faster as the scratch depth expands.

Data Availability

The data used to support the findings of this study are available from the corresponding author upon request.

Conflicts of Interest

The authors declare that there are no conflicts of interest regarding the publication of this article.

Acknowledgments

The authors gratefully acknowledge the support of the National Natural Science Foundation of China (No. 11272253), the Natural Science Foundation of Shaanxi Province (No. 2018JM5023, No. 2018JM1028, and No. 2018JM5119), and the Ph.D. Innovation Fund Projects of Xi'an University of Technology (Fund No. 310-252071702).

References

[1] K. Marynowski, "Non-Linear vibrations of the axially moving paper web," *Journal of Theoretical and Applied Mechanics*, vol. 46, no. 3, pp. 565–580, 2008.

[2] K. Marynowski, "Free vibration analysis of the axially moving Levy-type viscoelastic plate," *European Journal of Mechanics - A/Solids*, vol. 29, no. 5, pp. 879–886, 2010.

[3] Z. H. Li and Y. H. Li, "Muti-mode coupled transverse vibration of the plate," *Acta Materiae Compositae Sinica*, vol. 29, no. 3, pp. 219–225, 2012.

[4] Y.-Q. Tang and L.-Q. Chen, "Stability analysis and numerical confirmation in parametric resonance of axially moving viscoelastic plates with time-dependent speed," *European Journal of Mechanics - A/Solids*, vol. 37, pp. 106–121, 2013.

[5] Z. Pan, Z. Wang, and L. Fan, "Transversal vibration characteristics of moving viscoelastic rectangular plate with thermally induced varying physical parameters algorithm," *Yingyong Lixue Xuebao/Chinese Journal of Applied Mechanics*, vol. 32, no. 5, pp. 738–742, 2015.

[6] Y. Tang, D. Zhang, M. Rui, X. Wang, and D. Zhu, "Dynamic stability of axially accelerating viscoelastic plates with longitudinally varying tensions," *Applied Mathematics and Mechanics-English Edition*, vol. 37, no. 12, pp. 1647–1668, 2016.

[7] M. T. Robinson and S. Adali, "Effects of the thickness on the stability of axially moving viscoelastic rectangular plates," *Applied Acoustics*, vol. 140, pp. 315–326, 2018.

[8] M. T. Armand Robinson, "Analysis of the vibration of axially moving viscoelastic plate with free edges using differential quadrature method," *Journal of Vibration and Control*, vol. 24, no. 17, pp. 3908–3919, 2018.

[9] Y. F. Zheng and L. Q. Deng, "Nonlinear Free Vibration for Viscoelastic Moderately Thick Laminated Composite Plates with Damage Evolution," *Mathematical Problems in Engineering*, vol. 2010, Article ID 562539, 15 pages, 2010.

[10] K. Marynowski, "Non-linear vibrations of an axially moving viscoelastic web with time-dependent tension," *Chaos, Solitons & Fractals*, vol. 21, no. 2, pp. 481–490, 2004.

[11] Y. F. Zhou and Z. M. Wang, "Vibrations of axially moving viscoelastic plate with parabolically varying thickness," *Journal of Sound and Vibration*, vol. 316, no. 1–5, pp. 198–210, 2008.

[12] Y.-F. Zhou and Z.-M. Wang, "Transverse vibration characteristics of axially moving viscoelastic plate," *Applied Mathematics and Mechanics-English Edition*, vol. 28, no. 2, pp. 209–218, 2007.

[13] T. Bose and A. R. Mohanty, "Vibration analysis of a rectangular thin isotropic plate with a part-through surface crack of arbitrary orientation and position," *Journal of Sound and Vibration*, vol. 332, no. 26, pp. 7123–7141, 2013.

[14] F. Diba, E. Esmailzadeh, and D. Younesian, "Nonlinear vibration analysis of isotropic plate with inclined part-through surface crack," *Nonlinear Dynamics*, vol. 78, no. 4, pp. 2377–2397, 2014.

[15] Z. Wang, Y. Wang, and X. Guo, "Dynamic stability of linearly varying thickness viscoelastic rectangular plate with crack and subjected to tangential follower force," *Applied Acoustics*, vol. 70, no. 6, pp. 845–856, 2009.

[16] P. V. Joshi, N. K. Jain, and G. D. Ramtekkar, "Effect of thermal environment on free vibration of cracked rectangular plate: An analytical approach," *Thin-Walled Structures*, vol. 91, pp. 38–49, 2015.

[17] P. V. Joshi, N. K. Jain, and G. D. Ramtekkar, "Analytical modeling for vibration analysis of thin rectangular orthotropic/functionally graded plates with an internal crack," *Journal of Sound and Vibration*, vol. 344, pp. 377–398, 2015.

[18] G. S. Ramtekkar, N. K. Jain, and P. V. Joshi, "Non-linear vibration analysis of isotropic plate with perpendicular surface cracks," in *Advances in Structural Engineering: Mechanics*, vol. 1, pp. 77–94, Springer, India, 2015.

[19] W. Flugge, *Viscoelasticity*, Springer, Berlin, Germany, 2nd edition, 1975.

[20] J. R. Rice and N. Levy, "The Part-Through Surface Crack in an Elastic Plate," *Journal of Applied Mechanics*, vol. 39, no. 1, p. 185, 1972.

[21] S. E. Khadem and M. Rezaee, "Analytical approach for obtaining the location and depth of an all-over part-through crack on externally in-plane loaded rectangular plate using vibration analysis," *Journal of Sound and Vibration*, vol. 230, no. 2, pp. 291–308, 2000.

[22] H. Hu and Y. M. Fu, "Linear free vibration of a viscoelastic plate with an all over part through crack," *Journal of Changsha University of Science and Technology (Natural Science)*, vol. 1, pp. 19–26, 2006.

[23] Ö. Civalek, "Application of differential quadrature (DQ) and harmonic differential quadrature (HDQ) for buckling analysis of thin isotropic plates and elastic columns," *Engineering Structures*, vol. 26, no. 2, pp. 171–186, 2004.